Surface magnetoelastic waves in the presence of exchange interactions and pinning of surface spins

R. E. Camley
Department of Physics, University of California, Irvine, California 92717

R. Q. Scott
McDonnel Douglas Astronautics Company, Huntington Beach, California 92647
(Received 30 January 1978)

We present a theoretical study of the propagation of surface magnetoelastic waves on a ferromagnetic crystal which includes the effect of the exchange energy and the pinning of surface spins. The magnetoelastic wave is in essence a Rayleigh wave modified by the magnetoelastic coupling. Large deviations from the Rayleigh-wave propagation characteristics are found in the frequency range where bulk spin waves propagate and where surface spin waves propagate. The deviations associated with the surface spin wave are very sensitive to both exchange and pinning conditions, while those associated with the bulk spin waves are insensitive.

I. INTRODUCTION

It is well known that ultrasonic waves in a ferromagnetic crystal may interact with the spin system to produce a magnetoelastic wave which is a combination of stress waves and spin waves. Through the magnetoelastic coupling, Rayleigh waves, elastic waves bound to the surface of the crystal, may interact strongly with both the bulk spin waves and the surface spin waves. This produces a magnetoelastic surface wave. The wavelength and penetration depth of this wave can be made small compared to sample dimensions and thus one may think of the wave as propagating on a semi-infinite medium. The behavior of the magnetoelastic wave is interesting in several respects. The wave may be used as a probe of the nature of the elastic and spin systems near the surface of the crystal. Also, the properties of the wave (attenuation rate, penetration depth, and dispersion) may be altered by external parameters such as the strength and direction of an applied magnetic field.

A number of theoretical studies of surface magnetoelastic waves have been made.[1-9] Typically the studies take the external magnetic field and the magnetization to lie parallel to the surface of the crystal. One then enquires into features of the magnetoelastic wave, such as dispersion and attenuation length, which propagates along the surface at some angle relative to the magnetic field.

The basic results of these studies are as follows: there exists a magnetoelastic wave which is Rayleigh-like in its lattice displacement patterns and which reduces to the Rayleigh wave in the limit of vanishing magnetoelastic coupling. The propagation wave vector is complex, so the wave is damped as it moves along the surface. In regions where the frequency and parallel wave vector of the Rayleigh wave are close to those of bulk spin waves, the damping is large. This is a result of the elastic system radiating its energy to the bulk spin waves. Damping is also significant in the frequency range of surface spin waves.

The propagation characteristics are strongly dependent on the angle between the applied magnetic field and the direction of propagation. When propagation is parallel to the field, there is significant damping over the entire range of allowed bulk spin wave frequencies. As the angle between the field and the direction of propagation is increased, the damping is limited to a smaller region of the bulk wave spectrum. Another interesting feature is the nonreciprocal nature of the wave, i.e., the wave which goes from right to left across the magnetic field has attenuation and velocity significantly different from one which goes left to right.

The effect of exchange and spin pinning was not included in any of the above studies. Since exchange energy is dependent on the gradient of the magnetization, one might reasonably expect that exchange effects might be appreciable in a wave with only a short penetration length. In fact the penetration lengths in the magnetoelastic wave are comparable to the thickness of the thin films used to measure exchange constants by the method of ferro-magnetic resonance.[10]

The analysis of the effect of exchange and pinning of surface spins on the magnetoelastic wave is interesting in that the waves should provide a useful tool for studying the nature of spin pinning interactions at the surface of a macroscopic ferromagnetic crystal. Most information about spin pinning at surfaces has come from studies of the ferromagnetic resonance spectrum of thin

films deposited on substrates, and not on single crystals.

In our results, we find the damping of the magnetoelastic wave due to the interaction with the surface spin waves to be very sensitive to pinning conditions. As pinning is increased the damping is reduced. Furthermore with the addition of exchange and pinning, the damping due to the surface spin wave occurs at a higher frequency. With the addition of exchange, the width of the surface spin wave attenuation peak is no longer controlled by $1/\tau$, where τ is the spin relaxation rate, but by the exchange constant. This is a consequence of introducing exchange and pinning into the equations of motion and boundary conditions which govern surface spin waves and reflect a change in the nature of the surface spin waves. The surface spin waves themselves are damped by radiating their energy to bulk waves. We find this radiative damping is the dominant source of linewidth for the surface magnetoelastic mode in the frequency range of the surface spin waves, for the parameters explored here.

The interaction between the bulk spin waves and Rayleigh waves is basically unaffected by the addition of exchange and pinning. However since the bulk spin wave band is extended by the exchange energy, damping due to this interaction now occurs over a larger frequency range.

II. THEORY

We consider an elastically isotropic semi-infinite ferromagnetic crystal. The crystal occupies the half-space $y>0$. The external constant magnetic field $\vec{H}_0$ and the magnetization $\vec{M}_s$ are taken to be in the z direction which is parallel to the surface. The wave propagates with frequency Ω and wave vector $Q_{\parallel}$ ($Q_{\parallel}$ is parallel to the surface), at angle θ relative to the x axis. This geometry is shown in Fig. 1.

The equations of motion for the spin system in the absence of magnetoelastic coupling are

$$\frac{dM_x}{dt}=\gamma(\vec{M}\times\vec{H})_x - D\nabla^2 M_y - \frac{M_x}{\tau}\,, \tag{1}$$

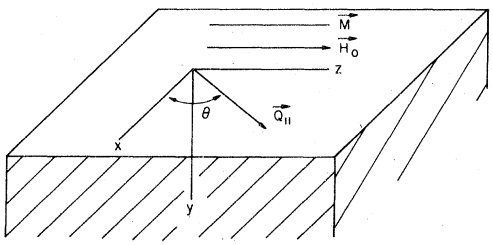

FIG. 1. Propagation geometry considered in this paper. The magnetization of the ferromagnet is parallel to the surface as is the externally applied constant magnetic field.

$$\frac{dM_y}{dt}=\gamma(\vec{M}\times\vec{H})_y + D\nabla^2 M_x - \frac{M_y}{\tau}\,, \tag{2}$$

where γ is the gyromagnetic ratio, τ is the transverse spin relaxation time, and D is the exchange constant. $\vec{H}$ is given by

$$\vec{H}=H_0\hat{z}+\vec{h}_d\,, \tag{3}$$

where H_0 is the applied field and $\vec{h}_d$ is the demagnetizing field set up by the spin motion.

The field $\vec{h}_d$ is calculated from Maxwell's equations. Here we use the magnetostatic approximation for Maxwell's equations:

$$\nabla\cdot\vec{B}=\nabla\times\vec{H}=0\,. \tag{4}$$

This is acceptable since in acoustical systems the frequency is limited to a few GHz. This gives us wave vectors on the order of 10^5 cm^{-1}. Thus $cQ\gg\Omega$, where c is the speed of light, and retardation effects may be ignored.

The equations of motion for the elastic system are

$$\rho\frac{\partial^2 u_k}{\partial t^2}=\sum_i \frac{\partial}{\partial x_i}\left(\frac{\partial\mathcal{H}}{\partial e_{ki}}\right), \tag{5}$$

where u_k is the kth component of the elastic displacement, $\mathcal{H}$ is the Hamiltonian density for an isotropic elastic solid, and

$$e_{ki}=\frac{1}{2}\left(\frac{\partial u_k}{\partial x_i}+\frac{\partial u_i}{\partial x_k}\right) \tag{6}$$

are elements of the strain tensor.

We now modify these equations by including terms resulting from the magnetoelastic coupling. The Hamiltonian density from the coupling for a ferromagnetic crystal with cubic symmetry in the spin-wave regime is given by

$$\mathcal{H}_{ls}=(b_2/M_s)[M_x(e_{xz}+e_{zx})+M_y(e_{yz}+e_{zy})]\,. \tag{7}$$

The term M_s is the saturization magnetization, and b_2 is a phenomenological coupling constant.[11]

The effect of this interaction Hamiltonian density in the spin equations of motion appears as an effective magnetic field $\vec{h}_{ls}$, where

$$\gamma\vec{h}_{ls}=-(\hat{x}\,b_2/M_s)(e_{xz}+e_{zx})-(\hat{y}\,b_2/M_s)(e_{yz}+e_{zy}); \tag{8}$$

in the lattice equations of motion the effect of the interaction energy is given by adding $\mathcal{H}_{ls}$ to $\mathcal{H}$:

$$\frac{dM_x}{dt}=\gamma[\vec{M}\times(\vec{H}+\vec{h}_{ls})]_x - D\nabla^2 M_y - \frac{M_x}{\tau}\,, \tag{9}$$

$$\frac{dM_y}{dt}=\gamma[\vec{M}\times(\vec{H}+\vec{h}_{ls})]_y + D\nabla^2 M_x - \frac{M_y}{\tau}\,, \tag{10}$$

$$\nabla\cdot\vec{B}=\nabla\times\vec{H}=0\,, \tag{11}$$

$$\frac{\partial^2 u_k}{\partial t^2} = \frac{1}{\rho}\sum_i \frac{\partial}{\partial x_i}\frac{\partial(\mathcal{H}+\mathcal{H}_{ls})}{\partial e_{ki}}. \tag{12}$$

We look for solutions of these equations of motion to be surface waves. The y variation of all dynamical variables is exponentially damped with a rate α. Thus,

$$u_x = u_{x0}\, e^{-\alpha y} e^{i(Q_x x + Q_z z)} e^{-i\Omega t}, \tag{13}$$

and similar expressions hold for u_y, u_z, M_x, M_y, and h_z. We have chosen h_z, the $\hat{z}$ component of the demagnetizing field $\vec{h}_d$, as the sixth dynamical variable.

Outside in the region $y<0$ one must only satisfy

$$\nabla\cdot\vec{B} = \nabla\times\vec{H} = 0, \tag{14}$$

assuming that the wave outside varies as

$$e^{+\alpha_0 y} e^{i(Q_x x + Q_z z)} e^{-i\Omega t}, \tag{15}$$

one can show through Eq. (14) that $\alpha_0^2 = Q_\parallel^2$.

We transform the lattice displacement coordinates to

$$u_x = u_l\cos\theta - u_t\sin\theta, \tag{16}$$

$$u_y = u_\perp, \tag{17}$$

$$u_z = u_l\sin\theta + u_t\cos\theta, \tag{18}$$

where u_l and u_t are the longitudinal and transverse components of displacement on the surface which are parallel and perpendicular to $Q_\parallel$. $u_\perp$ is the component of displacement normal to the surface.

Making these changes one obtains the following set of equations, arranged in matrix form:

$$\begin{bmatrix}
\frac{-i\gamma M_s\alpha}{Q_\parallel\sin\theta} & -\gamma b_2\alpha\sin\theta & i\gamma b_2 Q_\parallel\sin\theta & -\gamma b_2\alpha\cos\theta & i\left(\Omega+\frac{i}{\tau}\right) & \gamma H_0 + D(Q_\parallel^2-\alpha^2) \\
\frac{-i\gamma M_s}{\tan\theta} & -\gamma b_2 Q_\parallel\sin 2\theta & 0 & -\gamma b_2 Q_\parallel\cos 2\theta & i[\gamma H_0 + D(Q_\parallel^2-\alpha^2)] & \Omega+\frac{i}{\tau} \\
0 & (\Omega^2 + c_t^2\alpha^2 - c_t^2 Q_\parallel^2) & -i(c_l^2-c_t^2)\alpha Q_\parallel & 0 & \frac{ib_2 Q_\parallel\sin 2\theta}{\rho M_s} & \frac{-b_2\alpha\sin\theta}{\rho M_s} \\
0 & i(c_l^2-c_t^2)\alpha Q_\parallel & -(\Omega^2 + c_t^2\alpha^2 - c_t^2 Q_\parallel^2) & 0 & 0 & \frac{-ib_2 Q_\parallel\sin\theta}{\rho M_s} \\
0 & 0 & 0 & (\Omega^2 + c_t^2\alpha^2 - c_t^2 Q_\parallel^2) & \frac{ib_2 Q_\parallel\cos 2\theta}{\rho M_s} & \frac{-\alpha b_2\cos\theta}{\rho M_s} \\
i(Q_\parallel^2-\alpha^2) & 0 & 0 & 0 & 4\pi i Q_\parallel^2\sin\theta\cos\theta & -4\pi Q_\parallel\alpha\sin\theta
\end{bmatrix}
\begin{bmatrix} h_z \\ u_l \\ u_\perp \\ u_t \\ M_x \\ M_y \end{bmatrix} = 0, \tag{19}$$

(19a) (19b) (19c) (19d) (19e) (19f)

where $Q_\parallel = (Q_x^2+Q_z^2)^{1/2}$ and c_l and c_t are the longitudinal and transverse sound velocities. In obtaining these equations, we have neglected second-order terms in the variables M_x, M_y, and h_z since in the spin-wave regime these variables are small quantities. Equation (19f) is the Maxwell equations combined into one statement.

The above set of equations has a solution only if the determinent of the coefficients is zero. This condition results in a polynomial of twelfth-order in α. As it is virtually impossible to generate analytic expressions for the coefficients of the various powers of α, we have used a computer routine which, given Ω and $Q_\parallel$, numerically finds the coefficients of each power of α. The roots of the polynomial are then also found. Of the twelve roots, six have real parts less than zero. These correspond to exponentially increasing solutions, and so must be discarded. From the remaining six roots, we construct a superposition of waves with different decay parameters. For example,

$$u_l = \sum_k u_{l0}^{(k)} e^{-\alpha_k y} e^{i(Q_x x + Q_z z)} e^{-i\Omega t}, \tag{20}$$

with similar expressions for the other variables. The amplitudes for a particular α_k are related through the bulk equations, and we can solve for $h_z^{(k)}$, $u_\perp^{(k)}$, $u_t^{(k)}$, $M_x^{(k)}$, and $M_y^{(k)}$ in terms of $u_l^{(k)}$. At this point only six arbitrary amplitudes remain, $u_l^{(1)}$ to $u_l^{(6)}$.

We now impose the boundary conditions upon these superposed solutions. The usual electromagnetic conditions of conservation of the normal components of $\vec{B}$ and the transverse components of $\vec{H}$ can be combined into one equation:

$$\left(\sum_k [(Q_\parallel^2)^{1/2} + \alpha_k] h_z^{(k)} - 4\pi i Q_\parallel\sin\theta\sum_k M_y^{(k)}\right)_{y=0} = 0; \tag{21}$$

by $(Q_\parallel^2)^{1/2}$ we mean the root for which the real part is positive. This result is a consequence of the field decaying as $\exp[y(Q_\parallel^2)^{1/2}]$ outside the

substrate ($y<0$). Note that since $Q_{\parallel}$ is complex, the term $(Q_{\parallel}^2)^{1/2}$ is also complex.

The elastic boundary conditions are that the surface be stress free. The relevant elements of the stress tensor t_{iy} must be set to zero at the surface. We obtain

$$t_{xy}=\left.\frac{\partial(\mathcal{H}+\mathcal{H}_{1s})}{\partial e_{xy}}\right|_{y=0}=\left.2c_{44}e_{xy}\right|_{y=0}=0, \tag{22}$$

$$t_{yy}=\left.\frac{\partial(\mathcal{H}+\mathcal{H}_{1s})}{\partial e_{yy}}\right|_{y=0}$$

$$=\left.c_{11}e_{yy}+c_{12}(e_{xx}+e_{zz})\right|_{y=0}=0, \tag{23}$$

$$t_{zy}=\left.\frac{\partial(\mathcal{H}+\mathcal{H}_{1s})}{\partial e_{zy}}\right|_{y=0}=\left.2c_{44}e_{yz}+\frac{b_2M_y}{M_s}\right|_{y=0}=0; \tag{24}$$

note that Eq. (24) contains a contribution from the magnetoelastic interaction.

The remaining boundary condition describes the pinning of the surface spins. We use the phenomenological form

$$\lambda\frac{d\vec{M}}{dy}-\vec{M}=0. \tag{25}$$

For $\lambda=0$, the spins are pinned, i.e., the boundary condition reduces to $\vec{M}=0$ at the surface. For $\lambda\to\infty$, the boundary condition becomes $d\vec{M}/dy=0$, the appropriate condition for free spins at a surface.

We now substitute the superposed solutions found earlier into the boundary conditions and obtain the following set of equations:

$$\sum_{k=1}^{6}(-\alpha_k\cos\theta\,u_l^{(k)}+iQ_{\parallel}\cos\theta\,u_{\perp}^{(k)}+\alpha_k\sin\theta\,u_t^{(k)})_{y=0}=0, \tag{26}$$

$$\sum_{k=1}^{6}\left[i\left(\frac{c_l^2}{c_t^2}-2\right)Q_{\parallel}u_l^{(k)}-\alpha_k\left(\frac{c_l}{c_t}\right)^2u_{\perp}^{(k)}\right]_{y=0}=0, \tag{27}$$

$$\sum_{k=1}^{6}\left(-c_t^2\alpha_k\sin\theta\,u_l^{(k)}+ic_t^2Q_{\parallel}\sin\theta\,u_{\perp}^{(k)}-\alpha_kc_t^2\cos\theta\,u_t^{(k)}+\frac{b_2M_y^{(k)}}{M_s}\right)_{y=0}=0, \tag{28}$$

$$\sum_{k=1}^{6}(\lambda\alpha_k+1)M_x^{(k)}\Big|_{y=0}=0, \tag{29}$$

$$\sum_{k=1}^{6}(\lambda\alpha_k+1)M_y^{(k)}\Big|_{y=0}=0, \tag{30}$$

$$\sum_{k=1}^{6}\{[(Q_{\parallel}^2)^{1/2}+\alpha_k]\,h_z^{(k)}-4\pi iQ_{\parallel}\sin\theta\,M_y^{(k)}\}_{y=0}=0. \tag{31}$$

Since M_x, M_y, h_z, u_t, $u_{\perp}$ are uniquely known in terms of u_l, for a given k, these equations represent a set of six homogeneous equations in the variables $u_l^{(1)}$ to $u_l^{(6)}$. Setting the determinant of the coefficients of $u_l^{(1)}$ to $u_l^{(6)}$ equal to zero provides the condition which relates $Q_{\parallel}$ to Ω.

The procedure outlined above is carried out through the use of a computer routine. To do this, one chooses a real value for Ω and guesses a value for $Q_{\parallel}$. (Note that with Ω real, we expect $Q_{\parallel}$ to be complex in order to have a damped wave.) Given these values of $Q_{\parallel}$ and Ω the routine calculates the allowed values of α, the relationship of $u_t^{(k)}$ to the other dynamical variables for each root, and computes the value of the determinent $D(Q_{\parallel},\Omega)$ of the coefficients of $u_l^{(1)}$ to $u_l^{(6)}$ in the boundary conditions. The problem is thus to find the complex values of $Q_{\parallel}$ for which $D(Q_{\parallel},\Omega)$, also complex, is zero. This search can be efficiently done on a computer, and one can find the zeroes of $D(Q_{\parallel},\Omega)$ to high accuracy. From this one can calculate the dispersion relation, penetration depths, and detail the behavior of the fields for various angles of propagation. We discuss the results in Sec. III.

III. RESULTS

The parameters used in this calculation were those characteristic of YIG. We take

$$C_l=7.21\times10^5\ \text{cm/sec},\quad \rho=5.17\ \text{g/cm}^3,$$

$$4\pi M_s=1750\ \text{G},\quad (\Omega_H\tau)^{-1}=0.01;$$

$$C_t=3.85\times10^5\ \text{cm/sec},\quad b_2=6.4\times10^6\ \text{erg/cm}^3,$$

$$\gamma=1.759\times10^7\ \text{rad/secG},\ D/\gamma=4.55\times10^{-9}\ \text{cm}^2\,\text{G}.$$

The external magnetic field of 250G gives a frequency of $\Omega_H=\gamma H_0$ of 4.4×10^9 rad/sec.

In Fig. 2 we present a graph of $C_R\,\mathrm{Im}(Q_{\parallel})/\Omega$

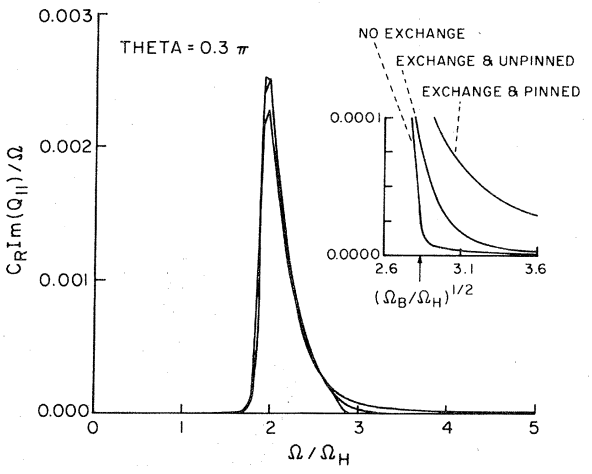

FIG. 2. Attenuation peak for the magnetoelastic wave when $\theta=0.3\pi$. We superimpose the results for three cases: no exchange, exchange and unpinned, and exchange and pinned. In the inset we show on expanded view of the curve near $(\Omega_B/\Omega_H)^{1/2}$, the top of the bulk spin-wave band in the limit of no exchange.

vs Ω/Ω_H. Since the dispersion relation for the Rayleigh wave is $\Omega = c_R k_{\parallel}$, the quantity $C_R\,\mathrm{Im}(Q_{\parallel})/\Omega$ represents the relative size of $\mathrm{Im}(Q_{\parallel})$ to the wave vector, $k_{\parallel}$ of the Rayleigh wave, and thus the relative damping of the magnetoelastic wave. In this graph we have superimposed the results for conditions of no exchange, exchange and unpinned, and exchange and pinning. The broad peak seen for all three conditions is largely unchanged by the introduction of exchange and pinning. This is because the shape of the peak is controlled by radiation of energy to the bulk spin waves and the position and width of the peak is dependent on their properties. (When we say the energy is radiated to the bulk spin waves we mean the energy is carried off by bulk magnetoelastic waves which have a strong admixture of spin wave character.)

In the frequency region of the peak, the exchange energy is small compared to the dipole energy, and the states of the bulk spin waves are not strongly changed by the exchange interaction. Also, one does not expect surface spin pinning to strongly affect the interior bulk spin states. Note, however, that for the condition of no exchange, the damping is limited to the frequency region where spin waves propagate. When the exchange energy is introduced, the spin wave spectrum is extended and the range of damping of the magnetoelastic wave is also extended.

In Fig. 3 we again graph $C_R\,\mathrm{Im}(Q_{\parallel})/\Omega$ for various conditions of exchange and pinning. Here θ is 0.5π so the wave travels parallel to the applied field. We note again that the large peak is only slightly changed by pinning and exchange. In a previous paper[7] it was shown that in the absence

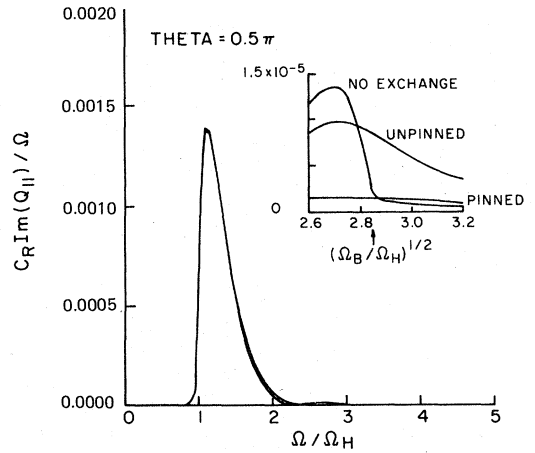

FIG. 3. Attenuation peak for $\theta = 0.5\pi$ for the three cases of no exchange, exchanged and unpinned, and exchange and pinned. In the inset we again show behavior near $(\Omega_B/\Omega_H)^{1/2}$.

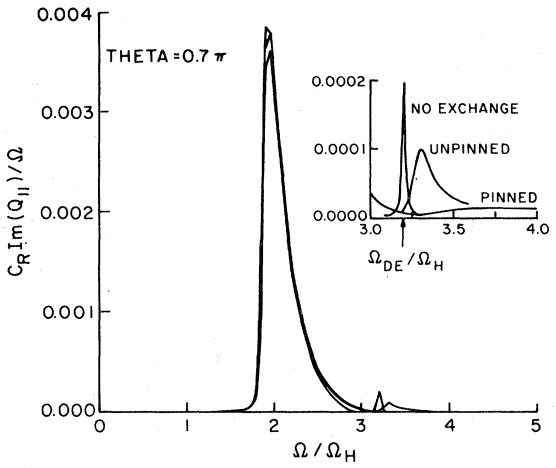

FIG. 4. Attenuation peak for $\theta = 0.7\pi$ for the three cases of no exchange, exchange and unpinned, and exchange and pinned. In the inset we show the behavior of the attenuation constant for frequencies near the Damon-Esbach frequency Ω_{DE}. The small peaks are caused by the Rayleigh wave coupling to surface spin waves.

of exchange for waves parallel to the magnetic field one expects a large peak at Ω_H and a smaller peak near $(\Omega_H\Omega_B)^{1/2}$. Note that in the presence of exchange the structure at $(\Omega_H\Omega_B)^{1/2}$ is eliminated. Again this is due to the extension of the spin wave band which results from the exchange interaction.

Figure 4 shows attenuation versus frequency for $\theta = 0.7\pi$. There are several striking differences between this graph and the previous two. First the height of the main attenuation peak is increased significantly compared to that of the wave when $\theta = 0.3\pi$. This is an example of the nonreciprocal nature of the wave; the wave traveling from right to left across the magnetic field is more severely damped than one traveling left to right. This feature is independent of exchange and is discussed in previous papers.[8]

Another interesting feature in Fig. 4 is the presence of small peaks not seen in Figs. 2 and 3. These peaks are a result of coupling of the surface elastic wave to surface spin waves. Note that the behavior of this peak is very sensitive to exchange and pinning conditions.

At this point we briefly recall the properties of surface spin waves in the dipolar regime. In the absence of exchange, the surface spin wave, or Damon-Eshbach wave,[12] propagates at a frequency that is dependent only on the direction of the wave. It propagates only for θ in the range $\pi - \varphi_c$ to $\pi + \varphi_c$, where

$$\varphi_c = \cos^{-1}[(H/B)^{1/2}]. \tag{32}$$

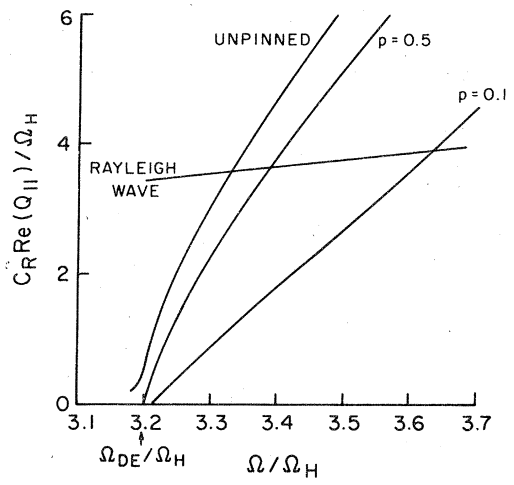

FIG. 5. Surface spin wave dispersion relation for $\theta = 0.7\pi$ as a function of pinning. The dimensionless parameter p is given by $\Omega_H \lambda / c_t$ so that as p increases the pinning has been decreased. Ω_{DE} is the Damon-Esbach frequency, i.e., the frequency of the surface spin wave in the limit of no exchange. Also shown is the dispersion relation for the Rayleigh wave.

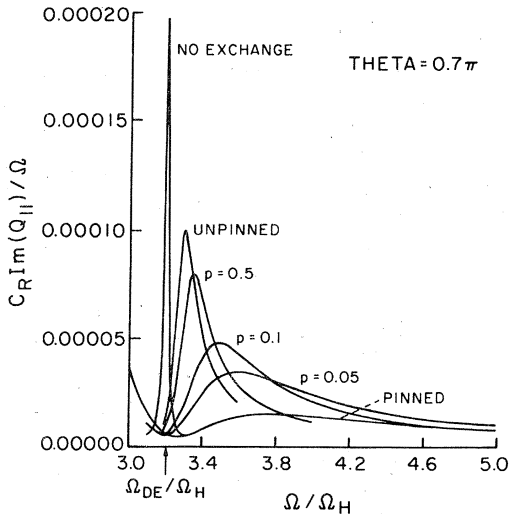

FIG. 6. Attenuation peak due to surface spin waves for various pinning constants. Again $p = \Omega_H \lambda / c_t$. The peak for no exchange is independent of pinning conditions.

The dispersion relation given by

$$\Omega_s(\theta) = -\tfrac{1}{2}(\Omega_H/\cos\theta + \Omega_B \cos\theta) \qquad (33)$$

is independent of the magnitude of $Q_{||}$. The factor $\Omega_B = \gamma B = \gamma(H_0 + 4\pi M_s)$. Note that at $\theta = \pi - \varphi_c$, $\Omega_s(\theta) = \gamma(HB)^{1/2}$, which is the top of the bulk spin-wave band. At $\theta = \pi$, $\Omega_s(\theta)$ reaches its maximum of $\frac{1}{2}(\Omega_H + \Omega_B)$.

When the effects of exchange energy and the pinning of surface spins are added into the surface spin-wave problem, the dispersion relation for the wave becomes dependent on the magnitude of Q as well as θ. The single frequency allowed before becomes a band of frequencies. The shape of the disperison curve is strongly dependent on surface spin pinning. The wave is damped as it moves along the surface due to a loss of energy to the bulk spin waves.

In Fig. 5 we present a graph of $C_R \mathrm{Re}(Q_{||})/\Omega_H$ vs Ω/Ω_H for the surface spin wave when exchange is included. To generate this curve, we set the magnetoelastic coupling constant to zero and apply the methods above to only the spin system. The graph for $\theta = 0.7\pi$ shows the effect of various pinning parameters. Also the dispersion relation for the bare Rayleigh wave, uncoupled to the spins, is drawn.

We can now explain the behavior of the peaks in the inset of Fig. 4. The sharp peak which occurs in the case of no exchange results from the Rayleigh wave driving the spin system in a resonant manner. The spin damping causes a dissipation of energy (heating). Note that for the case of no exchange, the width of the peak is equal to $1/\tau$. When exchange is added, the peak is both broadened and shifted. In this case the Rayleigh wave radiates its energy to the surface spin system similarly to the way it radiates energy to the bulk spin system. Note from Fig. 5 that the attenuation peak in the magnetoelastic wave occurs when the frequency and parallel wave vector of the Rayleigh wave are close to those of the surface spin wave. This explains the shift in the position of the peak. The peak is broadened because the Rayleigh wave interacts with the surface spin wave over a range of frequencies, not just at the Damon-Eshbach frequency.

In Fig. 6 we show the shape of the attenuation peak due to the surface spin waves as a function of various pinning parameters for fixed exchange constant D. We see that as pinning is increased, the position of the peak shifts toward higher frequencies and the peak is broadened. Although this graph is for 0.7π, it is typical of results at other angles. Again these results may be understood in reference to Fig. 5. In Fig. 5 we see that the intersection of the Rayleigh wave dispersion curve and the surface spin-wave dispersion curve occurs at higher frequencies as pinning is increased, and thus the peak is shifted.

In Fig. 7 we show the attenuation peak due to the surface spin waves for various angles. These results are similar to those for the case of no exchange in that the height of the peak is large near the critical angle and becomes smaller as θ approaches π.

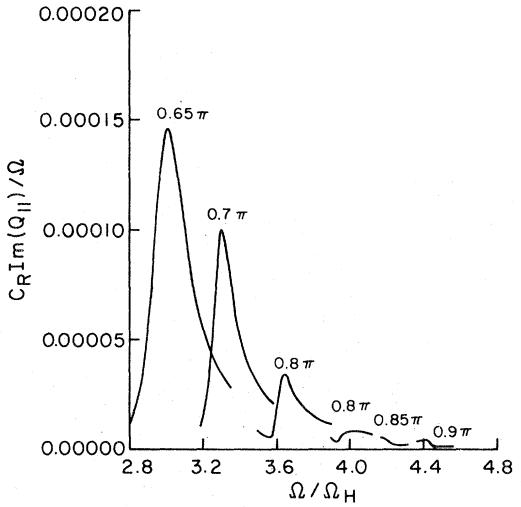

FIG. 7. Attenuation peak due to surface spin waves for various angles of propagation. Note that for the parameters used here θ_c, the smallest angle for which the surface spin wave exists in the limit of no exchange, equals 0.623π.

We explore the shape of the surface spin wave peak as a function of the spin damping constant in Fig. 8. The spin damping parameter used here is $\Gamma = 1/\Omega_H \tau$, where τ is the spin-relaxation time. In this graph we see that the height of the peak is sensitive to spin damping, but the width is insensitive. This indicates that the energy lost to the surface spin waves is primarily a radiative process similar to the loss of energy to bulk spin waves. Indeed, a similar graph made for the bulk spin wave peak shows analogous results; the height is sensitive to Γ but the width is not. With the

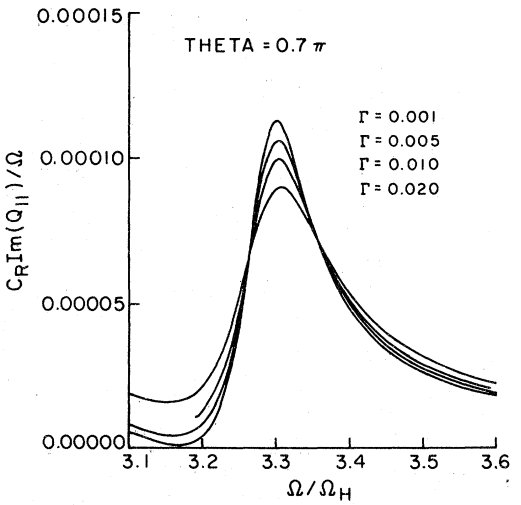

FIG. 8. Attenuation peak due to surface spin waves for various values of the transverse spin relaxation time τ; $\theta = 0.7\pi$. The dimensionless parameter $\Gamma = 1/\Omega_H \tau$.

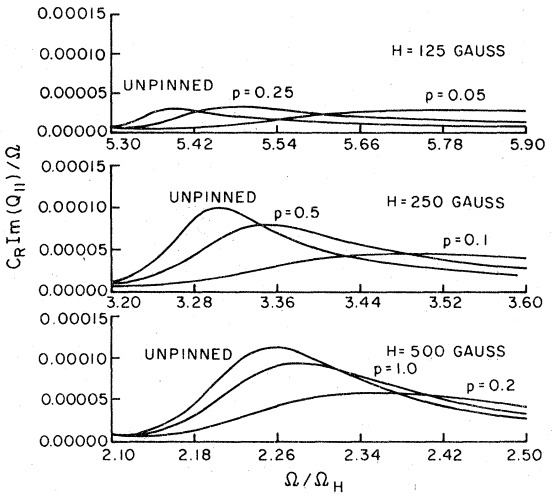

FIG. 9. Attenuation peak due to surface spin waves as a function of pinning constant and magnetic field strength. Again $p = \Omega_H \lambda / c_t$ and $\theta = 0.7\pi$.

addition of exchange, the width for both the bulk spin wave peak and the surface spin wave peak is controlled, not by Γ, but by the dispersion of the spin wave.

In Figs. 9 and 10 we present results on the behavior of both the surface and the bulk spin wave peaks for different magnetic-field values. In Fig. 9 at each field setting, several curves are drawn corresponding to different surface spin pinning conditions. We see that at each value of the field, pinning qualitatively effects the curve in the same way. With increasing pinning the peaks are shifted to higher frequencies and are

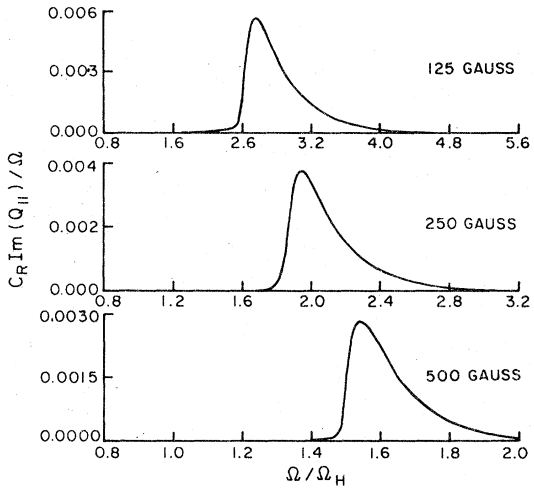

FIG. 10. Attenuation peak due to bulk spin waves for various magnetic field strength; $\theta = 0.7\pi$. Although we show only the unpinned case here, the effect of pinning on these graphs is virtually unnoticeable.

TABLE I. Absolute attenuation lengths (cm).

Magnetic field (G)	Bulk waves	Surface waves		
		Unpinned	$\lambda = 4.37 \times 10^{-5}$ cm	$\lambda = 8.75 \times 10^{-6}$ cm
500	0.0093	0.160	0.190	0.298
250	0.0109	0.246	0.303	0.488
125	0.0112	0.981	0.906	0.968

broadened. In Fig. 10 we draw only the unpinned case for the different field settings. The effect of the pinning of surface spins is unnoticeable.

It is interesting to note that as the magnetic field is increased, the relative height (i.e., the wavelength compared to damping length) of the peak due to bulk spin waves decreases, but the relative height of the peak due to surface spin waves increases. In Table I we compare the absolute attenuation lengths for the various cases. Note that even though the attenuation due to the surface spin waves is less than that due to bulk waves, it still damps the magnetoelastic wave significantly. In all cases the absolute attenuation length decreases with increasing field strength.

Thus we have seen that the elastic system interacts with both bulk spin waves and surface spin waves. In regions where the interaction is strong the resulting magnetoelastic wave is damped. Introducing exchange interactions and pinning of surface spins primarily effects the surface spin wave system. This is reflected in the magnetoelastic wave by an increase in the width of the attenuation peak associated with surface spin waves.

ACKNOWLEDGMENT

This research was supported by the U.S. Army Research Office, Durham, under ARO Grant No. DAAG29-77-G-0101.

[1]A wide variety of geometries and boundary conditions have been investigated but none, until the present work, has yet included the effect of exchange. Parekh and his collaborators have discussed surface magnetoelastic waves for both free surfaces and those loaded with a massless conducting layer. For a variety of propagation geometries, Scott and Mills have investigated surface magnetoelastic waves for arbitrary angles of propagation relative to the magnetic field. Emtage has discussed propagation perpendicular to the magnetic field and has included effects of magnetic and elastic anisotropy.

[2]J. P. Parekh, *Proceedings of the 1972 IEEE Ultrasonics Symposium* (IEEE, Boston, 1972), p. 333.

[3]J. P. Parekh and H. L. Bertoni, Appl. Phys. Lett. 20, 362 (1972).

[4]S. Shen, J. P. Parekh, and G. Thomas, *Proceedings of the 1974 IEEE Ultrasonics Symposium* (IEEE, New York, 1974), p. 483.

[5]J. P. Parekh, Electron. Lett. 6, 430 (1970).

[6]J. P. Parekh and H. L. Bertoni, J. Appl. Phys. 45, 434 (1974).

[7]R. Q. Scott and D. L. Mills, Solid State Commun. 18, 849 (1976).

[8]R. Q. Scott and D. L. Mills, Phys. Rev. B 15, 3545 (1977).

[9]P. R. Emtage, Phys. Rev. B 13, 3063 (1976).

[10]A good example of this type of measurement is found in J. T. Yu, R. A. Turk, and P. E. Wigen, Phys. Rev. B 11, 420 (1975).

[11]C. Kittel, Phys. Rev. 110, 836 (1958).

[12]R. W. Damon and J. R. Eshbach, J. Phys. Chem. Solids 19, 308 (1960).